Video Article

Measurement of Ultrafast Vibrational Coherences in Polyatomic Radical Cations with Strong-Field Adiabatic Ionization

Derrick Ampadu Boateng[1], Katharine Moore Tibbetts[1]

[1]Department of Chemistry, Virginia Commonwealth University

Correspondence to: Katharine Moore Tibbetts at kmtibbetts@vcu.edu

URL: https://www.jove.com/video/58263
DOI: doi:10.3791/58263

Keywords: Chemistry, Issue 138, Femtochemistry, pump-probe experiment, mass spectrometry, coherent control, vibrational wave packet, strong-field ionization, radical cation, molecular physics

Date Published: 8/6/2018

Citation: Ampadu Boateng, D., Tibbetts, K.M. Measurement of Ultrafast Vibrational Coherences in Polyatomic Radical Cations with Strong-Field Adiabatic Ionization. *J. Vis. Exp.* (138), e58263, doi:10.3791/58263 (2018).

Abstract

We present a pump-probe method for preparing vibrational coherences in polyatomic radical cations and probing their ultrafast dynamics. By shifting the wavelength of the strong-field ionizing pump pulse from the commonly used 800 nm into the near-infrared (1200-1600 nm), the contribution of adiabatic electron tunneling to the ionization process increases relative to multiphoton absorption. Adiabatic ionization results in predominant population of the ground electronic state of the ion upon electron removal, which effectively prepares a coherent vibrational state ("wave packet") amenable to subsequent excitation. In our experiments, the coherent vibrational dynamics are probed with a weak-field 800 nm pulse and the time-dependent yields of dissociation products measured in a time-of-flight mass spectrometer. We present the measurements on the molecule dimethyl methylphosphonate (DMMP) to illustrate how using 1500 nm pulses for excitation enhances the amplitude of coherent oscillations in ion yields by a factor of 10 as compared to 800 nm pulses. This protocol may be implemented in existing pump-probe setups through the incorporation of an optical parametric amplifier (OPA) for wavelength conversion.

Video Link

The video component of this article can be found at https://www.jove.com/video/58263/

Introduction

Since the invention of the laser in 1960's, the goal of selectively breaking chemical bonds in molecules has been a longstanding dream of chemists and physicists. The ability to tune both laser frequency and intensity was believed to enable direct cleavage of a target bond through selective energy absorbance at the associated vibrational frequency[1,2,3,4]. However, early experiments found that intramolecular vibrational redistribution of the absorbed energy throughout the molecule often resulted in non-selective cleavage of the weakest bond[4,5]. It was not until the development of femtosecond pulsed lasers and the pump-probe technique[6] in the late 1980's that direct manipulation of coherent vibrational states, or "wave packets", enabled successful control over bond cleavage and other objectives[6,7,8]. Pump-probe measurements, wherein the "pump" pulse prepares an excited state or ion that is subsequently excited by a time-delayed "probe" pulse, remain one of the most widely used techniques for studying ultrafast processes in molecules[9,10,11,12,13,14,15,16,17,18,19,20].

A significant limitation to studying the ultrafast dissociation dynamics of polyatomic radical cations using pump-probe excitation coupled to mass spectrometric detection arises from nonselective fragmentation of the target molecule by the ionizing pump pulse at the Ti:Sapphire wavelength of 800 nm[21,22,23]. This excess fragmentation results from nonadiabatic multiphoton ionization and can be mitigated by shifting the excitation wavelength into the near-infrared (*e.g.*, 1200-1500 nm)[22,23,24,25]. At these longer wavelengths, the contribution of adiabatic electron tunneling increases relative to multiphoton excitation in the ionization process[22,23]. Adiabatic tunneling imparts little excess energy to the molecule and forms predominantly "cold" ground state molecular ions[19,22,23]. Our previous work has demonstrated that the use of near-infrared excitation significantly improves the preparation of coherent vibrational excitations, or "wave packets", in polyatomic radical cations as compared to 800 nm excitation[19,20]. This work will illustrate the difference between strong-field ionization dominated by multiphoton and tunneling contributions with pump-probe measurements taken on the chemical warfare agent simulant dimethyl methylphosphonate (DMMP) using 1500 nm and 800 nm pump wavelengths.

In our pump-probe experiments, a pair of ultrashort laser pulses is time-delayed, recombined, and focused into a time-of-flight mass spectrometer, as shown in our setup in **Figure 1**. These experiments require a Ti:Sapphire regenerative amplifier producing >2 mJ, 800 nm, 30 fs pulses. The amplifier output is split on a 90:10 (%R:%T) beam splitter, where most of the energy is used to pump an optical parametric amplifier (OPA) for generation of 1200 - 1600 nm, 100 - 300 µJ, 20 - 30 fs pulses. The diameter of the IR pump beam is expanded to 22 mm and the diameter of the 800 nm probe beam down-collimated to 5.5 mm and cored using an iris. These collimations result in the pump beam focusing to a significantly smaller beam waist (9 µm) than the probe beam (30 µm), thereby ensuring that all ions formed during the ionizing pump pulse are excited by the time-delayed probe pulse. This configuration is used because the goal of our experiments is to probe the dynamics of the parent

molecular ion, which may be formed even at lower intensities near the edges of the focused beam. We note that if the dynamics of more highly-excited ionic species are of interest, then the probe beam diameter should be made smaller than that of the pump.

The pump and probe pulses propagate collinearly and are focused into the extraction region of a Wiley-McLaren time-of-flight mass spectrometer (TOF-MS)[26] (**Figure 2**). Molecular samples placed in a vial are attached to the inlet and opened to the vacuum. This setup requires that the molecule under investigation have a nonzero vapor pressure; for molecules with low vapor pressure, the vial may be heated. The flow of gaseous sample into the chamber is controlled by two variable leak valves. The sample enters the chamber through a 1/16" stainless steel tube approximately 1 cm away from the laser focus (**Figure 2**) in order to deliver a locally high concentration of target molecule in the extraction region[27]. The extraction plate has a 0.5 mm slit oriented orthogonal to the laser propagation and ion paths. Because the Rayleigh range of the pump beam is approximately 2 mm, this slit serves as a filter, allowing only ions generated from the central focal volume where the intensity is highest to pass through the extraction plate[28]. The ions enter a 1 m field-free drift tube to reach the Z-gap micro channel plate (MCP) detector[29], where they are detected and recorded with a 1 GHz digital oscilloscope at the 1 kHz repetition rate of typical commercial Ti:Sapphire lasers.

Protocol

NOTE: All commercially acquired instruments and parts such as the laser, vacuum pumps, chamber, time-of-flight tube and microchannel plate detector were installed and operated according to the manufacturer's instructions or user's manual. Laser safety goggles designed for the operating laser intensities and wavelengths should be worn.

1. Construction of TOF-MS[26]

1. Design and build an ultrahigh vacuum (UHV) chamber that has enough space to accommodate a standard stack of ion optics[26] and provisions to mount optical windows on 2 ¾" flanges on either side of the ion optics (**Figure 1**).
2. Attach the stack of ion optics mounted on a 1-m flight tube to the chamber.
   Note: To save space on the optical table, it is easiest to mount the ion optics and flight tube vertically.
3. Insert a 1/16" stainless steel tube into the chamber between the extractor and repeller plates, thread the tube out of the chamber, and connect it to ¼" stainless steel tubing[27]. Attach one or more variable leak valves to the ¼" stainless steel tubing.
   Note: Glass tubes containing molecular samples or gas tanks may be attached to this tubing for sample inlet.
4. Attach an 18-mm microchannel plate stack in Z-stack configuration[29] on the end of the flight tube.
5. Attach two optical windows (1 mm thickness, 50 mm diameter, fused silica) mounted on 2 ¾" flanges to the chamber.
   Note: The laser beams propagate through these two windows through the space between the repeller and extractor plates.
6. Wire the ion optics and the detector to high-voltage power supplies via current feedthroughs and BNC cables.
7. Attach one turbomolecular pump to the chamber near the ion optics and a second pump to the end of the flight tube near the detector (**Figure 1**). Connect both pumps to an appropriate backing pump.
   CAUTION: When attaching a turbomolecular pump to the end of a vertically-mounted flight tube, take care to ensure that the TOF system does not lean to one side due to the weight of the pump. This issue can be mitigated by attaching the vacuum chamber to the optical table.
8. Turn on the pumps and wait 24 h. The pressure in the chamber should be below 10^{-8} torr with no sample. If pressure is high, check for leaks and tighten the nuts or bake the chamber until desired pressure is reached.

2. Construction of Optical Pump and Probe Paths

Note: A diagram of the pump and the probe optical paths is given in **Figure 1**.

1. Provision of femtosecond laser pulses
   note: Femtosecond laser pulses (800 nm) were provided by a commercial Ti:Sapphire regenerative amplifier source operated according to the manufacturer's manual.
   1. Turn the laser on and wait for about 30 min for it to stabilize.
   2. Position a 90:10 (%R:%T) beam splitter after the laser output to generate two replica, which will be used to construct the pump and probe beam lines. Check the laser power of both replicas to ensure adequate power delivery.
   3. Direct the reflected beam into the optical parametric amplifier (OPA) and optimize the output power using the procedures in the manual.

2. Preparation of the pump optical path
   1. Set the OPA software to select the desired wavelength.
   2. Direct the output beam from the OPA through the λ/2 wave plate (WP) and polarizer (P).
   3. Block the p-polarized beam and direct the s-polarized beam to the concave (f = -10 cm) and convex (f = 50 cm) mirrors to expand its diameter by a factor of 5.
   4. Direct the expanded beam to the dichroic mirror (DC).

3. Preparation of the probe optical path
   1. Direct the beam that passes through the 90:10 beam splitter to the convex mirror (f = 20 cm) and concave mirror (f = -10 cm) to reduce its diameter by a factor of 2.
   2. Direct the down-collimated beam to a hollow retro-reflector mounted on a motorized linear delay stage. Adjust the mounting knobs of the two flat mirrors prior to the retro-reflector to ensure that the beam position after the retro-reflector does not change when the stage is moved along its full travel range.
      Note: This ensures that the pump-probe spatial overlap will be maintained over the full scan range.
   3. Insert a tunable neutral density (ND) filter after the delay stage to attenuate the power of the probe pulse, insert an iris after the ND filter to adjust the beam diameter, and direct the beam to the dichroic mirror (DC).

4. Measurement of pump and probe pulse durations
   Note: The durations of the pump and probe pulses are measured with a home-built second harmonic generation-frequency resolved optical gating (SHG-FROG) setup. Details on the construction of a SHG-FROG setup, measurement process, and data retrieval algorithms are described elsewhere[30,31,32]. In our experiments, pulse durations out of the OPA are typically around 20 fs and that of the 800 nm pulse around 30 fs[19,20,27]. However, OPAs can introduce higher-order pulse distortions, so it may be necessary to implement pulse-compression using, for instance, chirped mirrors[10,11,12,13] or an acousto-optic modulator[16].
   1. Block either the pump or probe beam. Direct the remaining beam into the FROG with flat mirrors placed after the dichroic mirror that combines the pump and probe pulses.
   2. Ensure that the two beam replicates in the FROG overlap in the β-barium-borate (BBO) crystal. Adjust the beam alignment and delay stage until a third beam is visible between the two original beams.
   3. With an iris and a *f* = 10 cm lens, isolate and focus the beam into a fiber-optic mount connected to the spectrometer and computer.
   4. Collect the FROG scan and retrieve the pulse shape with the appropriate software and retrieval algorithm.
   5. Repeat steps 2.4.1-2.4.3 for the other beam. Remove the mirrors directing beams to the FROG.

5. Rough spatial overlap of the pump and probe beams
   Note: If both pump and probe beams are visible, step 2.5.1 may be skipped.
   1. Insert a 15 mm-diameter BBO crystal after the dichroic to double the wavelengths of both beams, thereby making them visible.
      Note: It is easiest to use an OPA wavelength of ~1200-1300 nm for this step to make an orange 600-650 nm beam that is easily distinguishable from the blue 400 nm probe beam. Take care to ensure that the most intense region of the pump beam passes through the center of the crystal. The crystal angle should be optimized such that both the orange and blue pulses are easily visible, although this angle may not correspond to the maximum intensity of a given color.
   2. Adjust the pump and probe beam alignments using the mirror mounts prior to the dichroic such that the beams propagate collinearly through the TOF-MS chamber and out from the other side.
      Note: The probe beam has a smaller diameter and should be centered in the middle of the pump beam.

6. Rough temporal overlap of pump and probe beams
   Note: The method described here is limited to the oscilloscope resolution and can only determine the zero-delay position to within several millimeters of travel on the delay stage.
   1. Place a fast photodiode detector a few centimeters in front of the window entrance to the TOF-MS chamber in the path of the pump and probe beams. Attach the detector cable to a digital oscilloscope and independently locate the signals of the pump and probe pulses.
   2. Adjust the position of the motorized delay stage on the probe line such that the pump and probe signals in the oscilloscope are temporally overlapped. If one signal is consistently in front (behind) the other in the oscilloscope, move the mounts holding the motorized delay stage to shorten or lengthen the path length as needed.
   3. Remove the photodiode detector.

3. Preliminary Measurements

Note: All data in our experiments were acquired using codes written in-house with commercial instrument control software (**Table of Materials**). All instrument driver software was obtained from the respective manufacturer.

1. Calibration of absolute peak intensity of the pump pulse[28]
   1. Block the probe beam and insert a *f* = 20 cm lens mounted on a manual linear translation stage directly before the entrance window to the mass spectrometer.
   2. Adjust the wave plate (WP) rotation angle (**Figure 1**) to maximize the power of the pump beam measured before the lens.
   3. Attach a tank of Xe gas to the TOF-MS chamber inlet and adjust the leak valve controlling gas flow into the chamber such that the pressure gauge reads between 5-10 x 10^{-8} torr. Ensure that the TOF-MS power supply voltages are off when adjusting sample pressure to avoid damage to the MCP detector due to pressure spikes.
   4. Connect the output cables from the MCP detector and from the laser signal delay generator to a digital oscilloscope. Set the oscilloscope to trigger off the laser signal.
   5. Turn on the TOF-MS power supply and check the voltages. Typical values of the voltages for V_1, V_2, V_3, and V_4 (**Figure 2**) are +4,190 V, +3,910 V, 0 V, and -3,000 V, respectively.
   6. Check for ion signals of Xe^+ (and higher charge states) in the oscilloscope directly or via a computer connected to the oscilloscope.
   7. Adjust the position of the manual translation stage holding the lens to maximize the total ion signal. This step ensures that the pump beam focus overlaps with the 0.5 mm slit shown in **Figure 2**.
   8. Record the Xe mass spectrum using the data acquisition software.
   9. Decrease the laser power by rotating the WP angle to obtain a power ~20 mW lower than the previously measured power.
   10. Repeat steps 3.1.8-3.1.9 until the laser power is too low to generate measurable Xe^+ signal. A total of 10-15 mass spectra at different laser powers should be recorded.
   11. Using appropriate data analysis software, follow the steps in reference 28 to identify the laser pulse energy corresponding to the absolute saturation intensity for Xe^+ (1.12 x 10^{14} W cm^{-2})[28]. This procedure provides an absolute intensity scale for any pump pulse energy used in further experiments.

2. Calibration of absolute peak intensity of the probe pulse[33]
   Note: Due to the weak probe pulse intensity, the Xe calibration method described in step 3.1 cannot be used. Instead, the probe intensity in the experiments may be estimated by measuring the spot size at the focal point with a digital camera[32], along with the pulse duration and energy.
   1. Block the pump beam and direct the probe beam along a straight path after the dichroic mirror using two flat mirrors.

2. Remove the focusing lens from its position adjacent to the chamber and place it in the probe beam path, ensuring that the probe beam passes through its center.
3. Minimize the probe beam energy using the variable ND filter and add additional ND filters to attenuate the pulse energy below ~100 nJ.
4. Place a compact CMOS camera on a manual linear translation stage and connect it to a computer with suitable data acquisition software. Mount the translation stage in the probe beam path with the camera centered near the focal spot of the beam. Locate the beam spot using the software program. Add ND filters and adjust the camera acquisition settings to prevent saturation of the CMOS detector.
5. Adjust the position of the translation stage to obtain the smallest, most intense laser spot. This location corresponds to the focus of the beam.
6. Acquire a camera image at the focus and fit the spot to a two-dimensional Gaussian function using appropriate data analysis software to determine the beam diameter.
7. Remove the mirrors directing the probe beam to the camera and return the focusing lens to its position in front of the TOF-MS.

3. Determination of pump-probe spatial and temporal overlap in the TOF-MS
Note: The completion of the protocol in step 3.1 is assumed. While Xe gas could be used as the sample to determine spatial and temporal overlap, it is recommended to use the target molecule for study because changes in the mass spectrum can be observed over a range of positive time-delays instead of only at zero time-delay, as with Xe.
   1. Connect the desired sample to the TOF-MS chamber and adjust the pressure to the range of 1-5 x 10^{-7} torr.
   2. Unblock the pump and probe beams and ensure that they are aligned into the TOF-MS chamber.
   3. Maximize the probe power by adjusting the ND filter. Set the pump power with the waveplate to a sufficiently high level to obtain satisfactory ion signal.
      Note: The probe power should be sufficiently high to induce fragmentation but not so high as to create ions in the absence of the pump pulse.
   4. Adjust the spatial position of the probe beam with the knobs on the dichroic mirror mount (DC, **Figure 1**) until either a spike in intensity of all ions is observed (if the stage position is exactly at zero delay) or a significant depletion of the parent molecular ion and/or increase in fragment ion yields are observed (if the stage position corresponds to a positive time-delay).
   5. If no changes in the ion signals are observed, the stage position is likely at negative time-delay, *i.e.*, probe precedes pump. Adjust the motorized delay stage to a longer path for the probe beam and repeat step 3.3.4 until a change in the mass spectrum is observed.
   6. Adjust the motorized delay stage position to produce a spike in total ion signal. This position corresponds to zero time-delay. Representative mass spectra of the molecule DMMP taken at zero time-delay with good and poor spatial overlap, along with the mass spectrum taken with only the pump beam, are shown in **Figure 3**.

4. Cross-correlation[6,34]
Note: The cross-correlation measurement must be performed on an inert gas such as Xe[32]. It serves to verify both the pulse durations measured with FROG and the delay stage position corresponding to zero time-delay.
   1. With Xe gas in the chamber (step 3.1) and the beam overlap optimized (step 3.3), move the motorized stage position to locate zero time-delay (*i.e.*, when Xe^+ signal is maximized).
   2. Scan the motorized translation stage over the delay range of -200 fs to +200 fs in steps of 5 fs. This scan corresponds to steps of 1.5 µm over a range of 120 µm centered at the zero time-delay position. Record mass spectrum at each scan position and integrate Xe^+ yields to acquire the time-dependent ion signal[34].

4. Pump-probe Measurements

1. Preliminary checks before taking measurements
   1. Check the experimental setup to confirm that both beams are propagating collinearly through the window of the chamber (**Figure 1**).
   2. Attach the desired sample to the TOF-MS chamber and gradually release the sample into the chamber using variable leak valve(s) to achieve a target pressure of 1-5 x 10^{-7} torr. Ensure that the TOF-MS power supply voltages are turned off when adjusting the sample pressure to avoid damage to the MCP detector due to pressure spikes.
   3. If the vapor pressure of the molecule is too low to produce the desired pressure, gently heat the sample holder until desired pressure is achieved.
   4. Turn on and check TOF-MS voltages (step 3.1.5). Verify the operability of the data acquisition software with respect to the communication with both the motorized delay stage and oscilloscope.
   5. Adjust the lens in front of the chamber (step 3.1.7) and pump-probe spatial alignment (step 3.3.4) to optimize ion signal and spatial overlap.

2. Data acquisition
   1. Adjust the pump and probe pulse energies to obtain desired ion signals.
   2. In the data acquisition software, specify the scan length and step size.
      Note: Typical scan lengths in our experiments range from 1000-5000 fs and step sizes range from 5-20 fs[19,20].
   3. Run the data acquisition software to acquire the mass spectrum at each pump-probe delay.
      Note: Typically, the mass spectrum recorded at each time-delay in a scan is averaged over 1000 laser shots. To obtain sufficiently high signal-to-noise ratios, 10-20 scans are taken at the desired settings *(i.e.*, scan length, step size, pump and probe powers) and averaged. To minimize the effects of laser power drift, scans may be taken in alternating directions of delay-stage travel. All data are saved as tab-delimited text files. Representative raw mass spectral data from a single scan taken on DMMP for a scan length of 1250 fs with step size of 5 fs are shown in **Figure 4**.

3. Data processing
   1. Identify the flight time range for each mass peak of interest (illustrated by the bracketed regions in **Figure 4**) and integrate over these ranges in each mass spectrum. The outputs represent the time-resolved signals of each ion of interest. For example, time-resolved ion

signals of DMMP parent molecular ion with good and poor pump-probe spatial overlap obtained from one pump-probe scan are shown in **Figure 5**.

2. Repeat step 4.3.1 to obtain the desired number of scans (*e.g.*, 10-20)[19,20] at the same scan settings. Average each time-resolved ion signal over all scans taken. Representative averaged ion signals are shown in **Figure 6**.

Representative Results

Results obtained for the molecule DMMP[21] are presented. **Figure 3** shows the DMMP mass spectra taken at zero time-delay with the peak intensities of the 1500 nm pump and 800 nm probe pulses being 8 x 10^{13} and 8 x 10^{12} W cm^{-2}, respectively. For reference, the mass spectrum taken with only the pump pulse is also shown. The spectra are averaged over 10,000 laser shots (total acquisition time 12 s). The increase in ion signals marked with * is apparent when the spatial overlap between pump and probe beams is optimized (green spectrum). There is little perceptible difference between the poorly-overlapped and pump-only spectra. These results illustrate how to determine optimal spatial overlap of the pump and probe beams (step 3.3) using the ion signals directly.

Figure 4 shows mass spectral data obtained from one pump-probe scan (1000 laser shots/time step; 5 fs time steps; 1250 fs scan length), with the flight time on the abscissa and pump-probe delay on the ordinate. Total data acquisition time was approximately 16 min. The raw data illustrates how changes in ion signals with the pump-probe delay in these experiments can be visualized without additional data workup.

Figure 5 shows time-resolved $DMMP^+$ signals from one pump-probe scan (1000 laser shots/time step; 5 fs time steps; 2200 fs scan length; total acquisition time 16 min) with optimized (green) and poor (red) spatial overlap of pump and probe beams. These results illustrate the importance of optimizing the pump-probe spatial overlap (step 3.3) to acquire high-quality transient ion signals in the processed data.

Figure 6 shows $DMMP^+$ and the fragment $PO_2C_2H_4^+$ transient ion signals taken using 800 nm and 1500 nm pump wavelengths (**Figure 6a** and **b**, respectively). Signals were averaged over 10 scans (1000 laser shots/time step; 5 fs time steps; 1250 fs scan length); total acquisition time was approximately 3 h for each measurement. **Figure 6c** shows the fast Fourier transform (FFT) of the $DMMP^+$ ion signals taken with 800 nm and 1500 nm pumps. The peak at 750 nm visible for the 1500 nm pump illustrates the frequency resolution under the scan settings used. The frequency resolution obtainable with FFT may be improved by increasing the scan length. These results illustrate how the pump wavelength determines the observable ion dynamics.

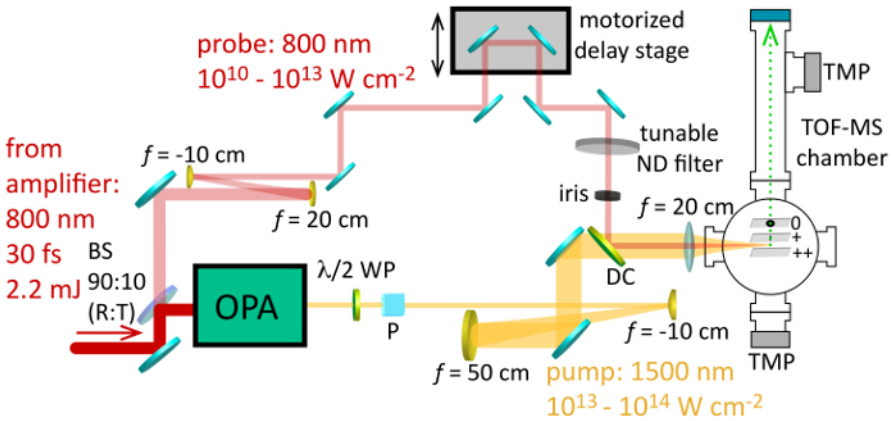

Figure 1: Optical pump-probe setup. The pump and probe beam paths are shown as yellow and red beams, respectively. Schematic diagrams of optical paths and guidance into the TOF-MS are shown. Abbreviations are as follows. BS: beam splitter (90:10, %R:%T). OPA: optical parametric amplifier. WP: λ/2 wave plate. P: polarizer cube. ND: neutral density. DC: dichroic. TMP: turbomolecular pump. Please click here to view a larger version of this figure.

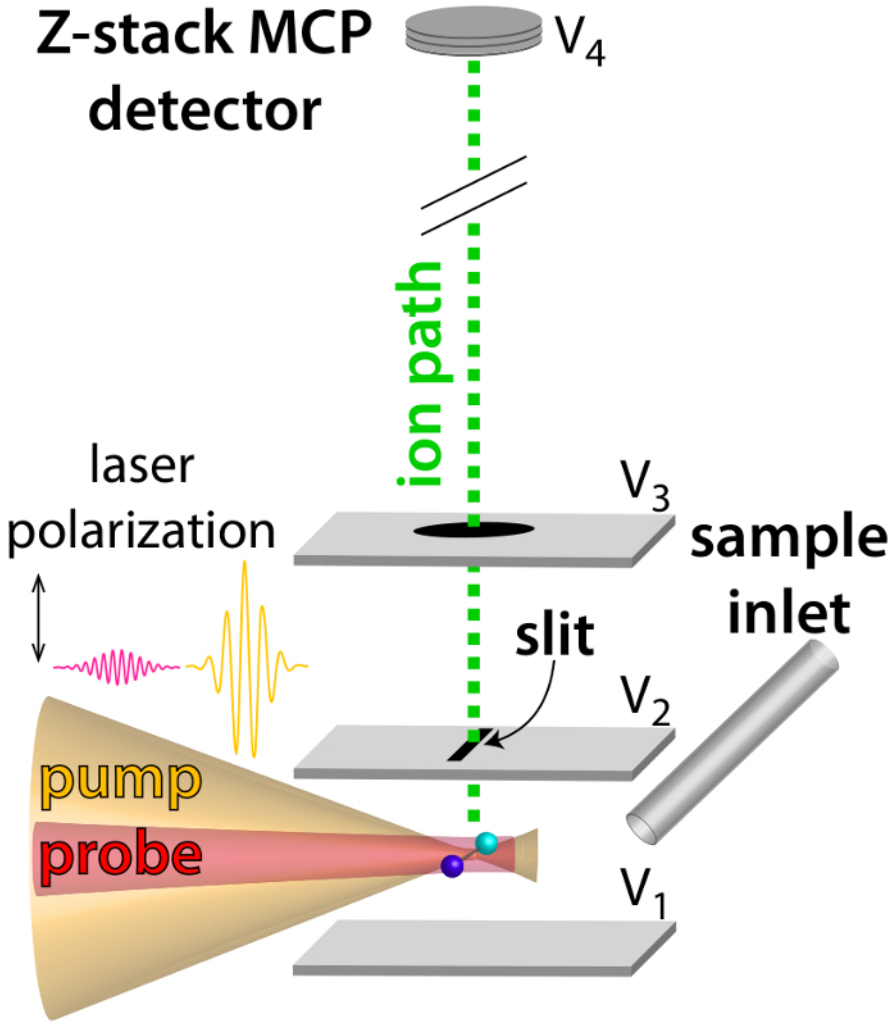

Figure 2: Schematic diagram of the laser-sample interaction region. Pump and probe beams are focused between the repeller (V_1) and extractor (V_2) plates. The polarization of both beams is aligned along the TOF axis. The voltages of the repeller plate (V_1 = +4190 V), extractor plate (V_2 = +3910 V), ground plate (V_3 = 0 V), and MCP detector bias (V_4 = -3000 V) are set in the TOF power supply. The 0.5 mm slit on the extractor plate is oriented perpendicular to both the laser and ion paths to ensure the collection of ions only from the most intense region of the laser focus[28]. The sample inlet tube is placed between the plates V_1 and V_2[27]. Please click here to view a larger version of this figure.

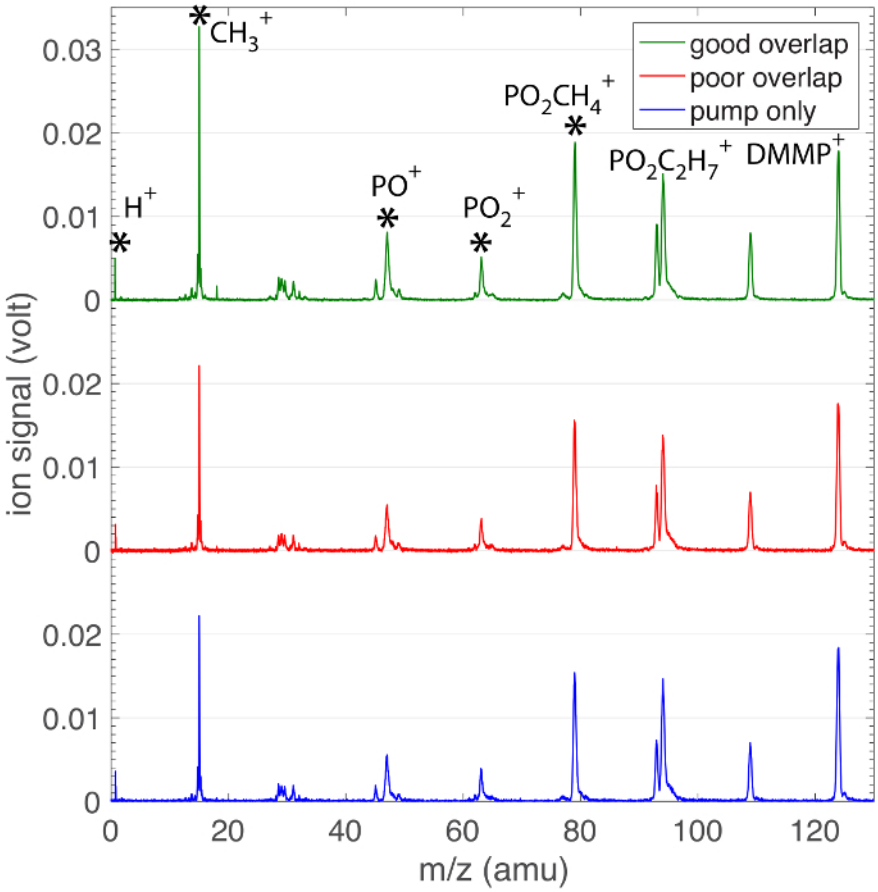

Figure 3: Mass spectra of DMMP. The sample molecule is DMMP and the spectra are taken at zero time-delay with good overlap (green) and poor spatial overlap (red). For reference, the spectrum taken with only the pump pulse (blue) is shown. Peaks marked with * denote ion signals that are enhanced when the spatial overlap is optimized. Please click here to view a larger version of this figure.

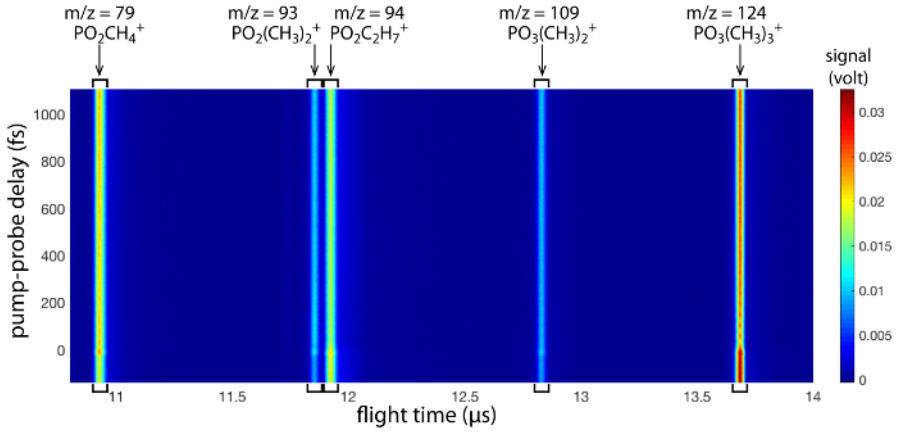

Figure 4: Raw pump-probe scan data. Mass spectral data recorded in the oscilloscope during one pump-probe scan at delays from -150 fs to +1100 fs. Flight time is labeled on the abscissa and pump-probe delay on the ordinate. The DMMP parent molecular ion and four fragment ion signals are labeled. Integration ranges for each ion signal are indicated by brackets. Please click here to view a larger version of this figure.

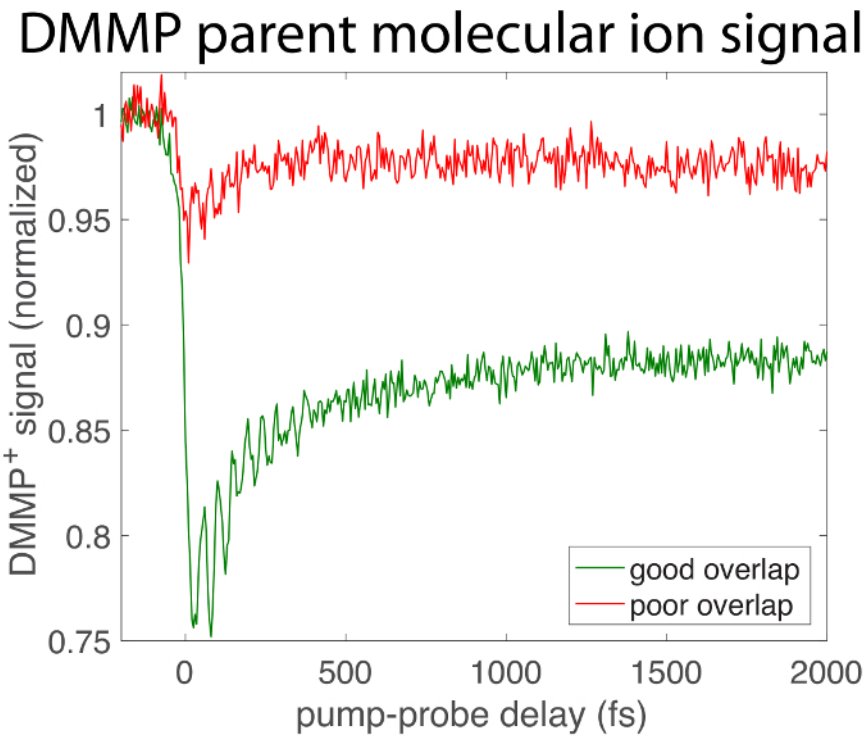

Figure 5: Pump-probe scan data with good and poor spatial overlap. The integrated signals of DMMP parent molecular ion obtained from a single scan taken with good overlap (green) and poor overlap (red) are plotted as a function of pump-probe delay. Please click here to view a larger version of this figure.

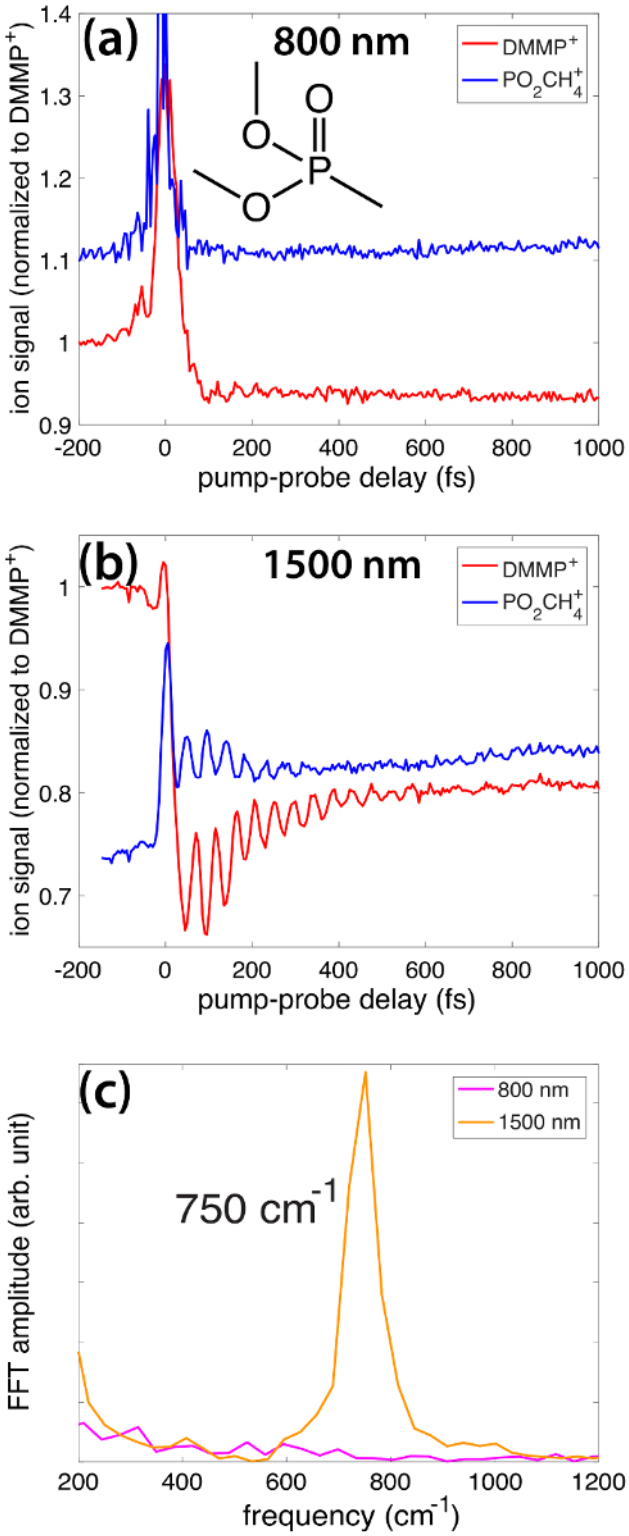

Figure 6: Effect of pump wavelength. Normalized $DMMP^+$ (red) and $PO_2CH_4^+$ (blue) ion signals as a function of pump-probe delay obtained for experiments using pump wavelengths of 800 nm (a) and 1500 nm (b). The FFT of each $DMMP^+$ ion signal is shown in panel (c). This figure has been adapted from reference 19 with permission from the PCCP Owner Societies. Please click here to view a larger version of this figure.

Discussion

This protocol enables us to resolve ultrafast vibrational dynamics in polyatomic radical cations through selective preparation of the ions in the ground electronic state. While the standard strong-field ionization procedure using 800 nm can prepare vibrational coherences in ground-electronic state radical cations of first-row diatomics[10,11,12,13] and CO_2[14,15], the population of multiple ionic excited states in polyatomic ions using

800 nm significantly limits the resolvable dynamics[17,19]. In DMMP (**Figure 6**), the amplitude of 45-fs coherent oscillations in the parent molecular ion yield is larger by a factor of ~10 when 1500 nm is used for ionization (red curve, **Figure 6b**) as compared to 800 nm (red curve, **Figure 6a**). Furthermore, large-amplitude oscillations in the fragment ion $PO_2CH_4^+$ are visible with a 1500 nm pump (blue curve, **Figure 6b**), but completely absent for 800 nm pump (blue curve, **Figure 6a**). Furthermore, FFT of the $DMMP^+$ ion signals (**Figure 6c**) shows a peak at 750 cm^{-1} resolvable to ~40 cm^{-1} when the pump wavelength is 1500 nm, while no peak is visible when the pump wavelength is 800 nm. These results illustrate the efficacy of strong-field adiabatic ionization for preparing radical cations in the ground electronic state with well-defined vibrational coherences.

A critical step in the protocol is to optimize the spatial overlap between pump and probe beams using the ion signals directly for feedback (step 3.3). The differences in the ion signals acquired using good and poor overlap are illustrated in **Figure 3** and **Figure 5**. While the fragmentation patterns will be different for each molecule, a reliable indicator of good spatial overlap is the enhancement of small-mass fragments in the mass spectrum, as seen in the peaks marked with a star in the green spectrum in **Figure 3** (good overlap) as compared to the red spectrum (poor overlap). The consequences of performing pump-probe scans (step 4.2) with good and poor spatial overlap are illustrated in **Figure 5**. When the overlap is good (green trace), six well-defined oscillations in the $DMMP^+$ yield are visible, with a relative depletion at 2000 fs delay of 12% from the yield at negative delay. When the overlap is poor (red trace), only two or three oscillations in $DMMP^+$ yield are visible and the relative depletion of the ion signal at 2000 fs delay is only 5% of the yield at negative delay. These results demonstrate the importance of operating with optimized spatial overlap in order to accurately record the ion dynamics.

The protocol described here has two limitations with regards to the molecules that may be easily studied. First, the effusive molecular beam inlet to the TOF-MS requires that the target molecules have a sufficiently high vapor pressure to go into the gas phase. Molecules with a lower vapor pressure, such as 4-nitrotoluene, may be gently heated to produce a sufficiently high pressure in the chamber to obtain satisfactory ion signals[20]. Second, many polyatomic molecules have low-lying ionic excited states that may be populated through resonant absorption during the pump pulse, even under adiabatic ionization conditions. For instance, acetophenone exhibits an ionic resonance at 1370 nm[24,25], which results in significantly decreased amplitudes in coherent oscillations in ion yields using this protocol[17]. Thus, the excitation wavelength for the pump must be chosen carefully to ensure a sufficiently high parent ion signal when only the pump is applied. For maximum flexibility, the use of a commercial OPA with the wavelength range of 1150-2500 nm is recommended.

This protocol has potential applications for chemical warfare agent and explosive detection, as illustrated in our studies on DMMP[19] and nitrotoluenes[20]. In addition to studies of coherent dynamics in radical cations, the use of near-infrared wavelengths for ionization has been used in pump-probe experiments to study ultrafast dynamics on neutral excited states in aminobenzonitriles[35], where the use of 1300-2100 nm ionizing probe pulses improved the resolution of ultrafast coherent oscillations in the ion yields. Thus, strong-field adiabatic ionization techniques may facilitate the study of a wide range of ultrafast dynamical processes in both neutrals and ions of polyatomic molecules.

Disclosures

The authors have nothing to disclose.

Acknowledgements

This work was supported by the U.S. Army Research Office through Contract W911NF-18-1-0051.

References

1. Letokhov, V.S. Photophysics and Photochemistry. *Physics Today.* **30**(5), 23-32 (1977).
2. Bloembergen, N., Yablonovitch E. Infrared laser induced unimolecular reactions. *Physics Today.* **31**(5), 23-30 (1978).
3. Zewail, A.H. Laser selective chemistry-is it possible? *Physics Today.* **33**(11), 25-33, (1980).
4. Brif, C., Chakrabarti, R.L., Rabitz, H. Control of quantum phenomena: past, present and future. *New Journal of Physics.* **12**, 075008 (2010).
5. Bloembergen, N., Zewail, A.H. Energy redistribution and the question of mode selective laser chemistry revisited. *The Journal of Physical Chemistry.* **88**(23), 5459-5465 (1984).
6. Rosker, M. J., Dantus, M., Zewail, A.H. Femtosecond real-time probing of reactions. I. The technique. *The Journal of Chemical Physics.* **89**(10), 6113-6127 (1988).
7. Zewail, A.H. Femtochemistry: Recent progress in studies of dynamics and control of reaction and their transition states. *The Journal of Physical Chemistry.* **100**(31), 12701-12724 (1996).
8. Warren, W.S., Rabitz, H., Dahleh, M. Coherent Control of Quantum Dynamics: The Dream Is Alive. *Science.* **259**(5101), 1581-1589 (2003).
9. Kosma, K., Trushin, S.A., Fuß, W., Schmid, E.E. Cyclohexadiene ring opening observed with 13 fs resolution: coherent oscillations confirm the reaction path. *Physical Chemistry Chemical Physics.* **11**(1), 172-181 (2009).
10. De, S., Magrakvelidze, M., Bocharova, I.A., Ray, D., Cao, W., Znakovskaya, I., Li, H., Wang, Z., Laurent, G., Thumm, U., Kling, M.F., Litvinyuk, I.V., Ben-Itzhak, I., Cocke, C.L. Following dynamic nuclear wave packets in N_2, O_2 and CO with few-cycle infrared pulses. *Physical Review A.* **84**(4), 043410 (2011).
11. Bryan, W.A., McKenna, J., English, E.M.L., Wood, J., Calvert, C.R., Torres, R., Murphy, D.S., Turcu, I.C.E., Collier, J.L., McCann, J.F., Williams, I.D., Newell, W.R. Isolated vibrational wavepackets in D_2^+: Defining superposition condition and wavepacket distinguishability. *Physical Review A.* **76**(5), 053402 (2007).
12. Calvert, C., Bryan, W., Newell, W., Williams, I. Time resolved studies of ultrafast wavepacket dynamics in hydrogen molecules. *Physics Reports.* **491**(1), 1-28 (2010).
13. Kelkensberg, F., Lefebvre, C., Siu, W., Ghafur, O., Nguyen-Dang, T.T., Atabek, O., Keller, A., Serov, V., Johnsson, P., Swoboda, M., Remetter, T., L'Huillier, A., Zherebtsov, S., Sansone,G., Benedetti, E., Ferrari, F., Nisoli, M., Lépine, F., Kling, M. F., Vrakking, M. J. J. Molecular dissociative ionization and wave-packet dynamics studied using two-color XUV and IR pump-probe spectroscopy. *Physical Review Letters.* **103**(12), 123005 (2009).

14. Erattupuzha, S., Larimian, S., Baltuska, A., Xie, X., Kitzler, M. Two-pulse control over double ionization pathways in CO_2. *The Journal of Chemical Physics.* **144**(2), 024306 (2016).
15. Rudenko, A., Makhija, V., Vajdi, A., Ergler, T., Schurholz, M., Kushawaha, R. K., Ullrich, J., Moshammer, R., Kumarappan, V. Strong field-induced wave packet dynamics in carbon dioxide molecule. *Faraday Discussions.* **194**, 463-478 (2016).
16. Pearson, J.B., Nichols, S.R., Weinacht, T., Molecular fragmentation driven by ultrafast dynamic ionic resonances. *The Journal of Chemical Physics.* **127**(13), 131101 (2007).
17. Bohinski, T., Tibbetts, K.M., Tarazkar, M., Romanov, D.A., Matsika, S., Levis, R.J. Strong field adiabatic ionization prepares a launch state for coherent control. *The Journal of Physical Chemistry Letters.* **5**(24), 4305-4309 (2014).
18. Tibbetts, K.M., Tarazkar, M., Bohinski, T., Romanov, D.A., Matsika, S., Levis, R.J. Controlling the dissociation dynamics of acetophenone radical cation through excitation of ground and excited state wavepacket. *The Journal of Physics B: Atomic, Molecular, and Optical Physics.* **48**(16), 164002 (2015).
19. Ampadu Boateng, D., Gutsev, G.L., Jena, P., Tibbetts, K.M. Ultrafast coherent vibrational dynamics dynamics in dimethyl methylphosphonate radical cation. *Physical Chemistry Chemical Physics.* **20**(7), 4636-4640 (2018).
20. Ampadu Boateng, D., Gutsev, G.L., Jena, P., Tibbetts, K.M., Dissociation dynamics of 3- and 4-nitrotoluene radical cations: Coherently driven C-NO_2 bond homolysis. *The Journal of Chemical Physics.* **148**(13), 134305 (2018).
21. Markevitch, A.N., Romanov, D.A., Smith, S.M., Schlegel, H.B., Ivanov, M.Y., Levis, R.J. Sequential non adiabatic excitation of large molecules and ions driven by strong laser fields. *Physical Review A.* **69**(1), 013401 (2004).
22. Lezius, M., Blanchet, M., Rayner, D.M., Villeneuve, D.M., Stolow, A., Ivanov, M.Y. Nonadiabatic multielectron dynamics in strong field molecular ionization. *Physical Review Letters.* **86**(1), 51 (2001).
23. Lezius, M., Blanchet, V., Ivanov, M.Y., Stolow, A. Polyatomic molecules in strong laser fields: Nonadiabatic multielectron dynamics. *The Journal of Chemical Physics.* **117**(4), 1575 (2002).
24. Bohinski, T., Tibbetts, K.M., Tarazkar, M., Romanov, D., Matsika, S., Levis, R.J. Measurement of an electronic resonance in a ground-state, gas-phase acetophenone cation via strong-field mass spectrometry. *The Journal of Physical Chemistry Letters.* **4**(10), 1587−1591 (2013).
25. Bohinski, T., Tibbetts, K.M., Tarazkar, M., Romanov, D., Matsika, S., Levis, R.J. Measurement of ionic resonance in alkyl phenyl ketone cations via infrared strong field mass spectrometry. *The Journal of Physical Chemistry A.* **117**(47), 12374-12381 (2013).
26. Wiley, W. C., & McLaren, I. H. Time-of-Flight Mass Spectrometer with Improved Resolution *Review of Scientific Instruments.* **26**, 1150-1156 (1955).
27. Gutsev, G. L., Ampadu Boateng, D., Jena, P., Tibbetts, K. M. A Theoretical and Mass Spectrometry Study of Dimethyl Methylphosphonate: New Isomers and Cation Decay Channels in a Femtosecond Laser Field. *The Journal of Physical Chemistry A.* **121**(44), 8414-8424 (2017).
28. Hankin, S.M., Villeneuve D.M., Corkum, P. B., Rayner, D.M. Intense-field laser ionization rates in atoms and molecules. *Physical Review A.* **64**(1), 013405 (2001).
29. Amitay, Z. and Zajfman, D. A new type of multiparticle three-dimensional imaging detector with subnanosecond time resolution. *Review of Scientific Instruments.* **68**(3), 1387-1392 (1997).
30. Trebino, R., Kane, D.J. Using phase retrieval to measure the intensity and phase of ultrashort pulses: frequency-resolved optical gating. *Journal of the Optical Society of America A.* **10**(5), 1101 (1993).
31. DeLong, K.W., Trebino, R., Hunter, J., White, W.E. Frequency-resolved optical gating with the use of second harmonic generation. *Journal of the Optical Society of America B.* **11**(11), 2206 (1994).
32. Trebino, R., *Frequency Resolved Optical Gating.* Kluwer Academy Publishers, Boston, (2000).
33. Ruff, J.A., Siegman, A.E. Single-pulse laser beam quality measurements using a CCD camera system. *Optics Letters.* **31**(24), 4907-4909 (1992).
34. Trushin, S.A., Kosma, K., Fuß, W., Schmid, W.E. Sub-10-fs supercontinuum radiation generated by filamentation of few-cycle 800 nm pulses in argon. *Optics Letters.* **32**(16), 2432-2434 (2007).
35. Fuß, W., Schmid, W.E., Pushpa, K.K., Trushin, S.A., Yatsuhashi, T. Ultrafast relaxation and coherent oscillations in aminobenzonitriles in the gas phase probed by intense-field ionization. *Physical Chemistry Chemical Physics.* **9**(10), 1151-1169 (2007).

